Synthesis of a Sulfido-Capped Trinuclear Cluster $[\{(\eta^5\text{-}C_5Me_5)Ir\}_2\{Mo(CO)_3\}(\mu_3\text{-}S)_2]$ and Its Reactions at the Molybdenum Site Forming a Series of Ir_2MoS_2 Clusters

Hidenobu Kajitani, Hidetake Seino, and Yasushi Mizobe*

Institute of Industrial Science, The University of Tokyo, Komaba, Meguro-ku, Tokyo 153-8505, Japan

Received February 28, 2007

Treatment of a hydrosulfido-bridged diiridium complex, $[(Cp^*IrCl)_2(\mu\text{-}SH)_2]$ (**1**; $Cp^* = \eta^5\text{-}C_5Me_5$), with $[Mo(\eta^6\text{-toluene})(CO)_3]$ in the presence of NEt_3 gave the sulfido-bridged Ir_2Mo cluster $[(Cp^*Ir)_2\{Mo(CO)_3\}(\mu_3\text{-}S)_2]$ (**3**). Detailed studies on the reactivity of its Mo site have resulted in the isolation of a series of new $Ir_2Mo(\mu_3\text{-}S)_2$ clusters. Thus, **3** reacted with $Ph_2PCH_2CH_2PPh_2$ (dppe) to afford $[(Cp^*Ir)_2\{Mo(CO)(dppe)\}(\mu_3\text{-}S)_2]$ (**4**), which underwent the oxidation by I_2 at the molybdenum site to give $[(Cp^*Ir)_2\{MoI(CO)(dppe)\}(\mu_3\text{-}S)_2]I$ (**5**). On the other hand, oxidation of **3** with $[Cp_2Fe][PF_6]$ in THF−MeCN resulted in the elimination of one CO ligand and concomitant coordination of two MeCN molecules at the Mo center, yielding $[(Cp^*Ir)_2\{Mo(CO)_2(MeCN)_2\}(\mu_3\text{-}S)_2][PF_6]_2$ (**6**). Further oxidation of **6** using O_2 gas led to the elimination of all the remaining CO ligands to give an oxo-dichloro cluster, $[(Cp^*Ir)_2(MoOCl_2)(\mu_3\text{-}S)_2]$ (**7**). The ligation of diphosphines to the molybdenum site in **7** formed the cationic oxo-chloro cluster $[(Cp^*Ir)_2\{MoOCl(R_2PC_2H_4PR_2)\}(\mu_3\text{-}S)_2]X$ (**8a**, R = Me (dmpe), X = Cl; **8b**, R = Et, X = Cl; **8c**, R = Ph, X = PF_6) with concurrent dissociation of one of the Cl ligands, and the following deoxygenation from **8a** with BCl_3 gave $[(Cp^*Ir)_2\{MoCl_3(dmpe)\}(\mu_3\text{-}S)_2][BCl_4]$ (**9**). Reduction of **9** with Cp_2Co afforded a paramagnetic Mo(III) cluster, $[(Cp^*Ir)_2\{MoCl_2(dmpe)\}(\mu_3\text{-}S)_2][BCl_4]$ (**11**), whereas reduction of **8c** with $NaBH_4$ resulted in the formation of a Mo(II) dihydrido cluster, $[(Cp^*Ir)_2\{MoH_2(dppe)\}(\mu_3\text{-}S)_2]$ (**12**). X-ray analyses have been undertaken to determine the detailed structures for **3**, **4**, **5**, **6**, **7**, **8b**, **9**, and **12**.

Introduction

Early−late heterobimetallic (ELHB) complexes have been attracting much attention because the cooperative action of early and late transition metals can display interesting synergistic effects on the reactions promoted by these mixed-metal sites.[1] To keep these multinuclear cores intact under required reaction conditions, incorporation of the bridging ligands that can firmly connect metal centers often becomes necessary. In this context, our studies have focused on the syntheses of mixed-metal clusters with bridging chalcogen ligands because of high bridging ability and strong affinity with transition metals, which are characteristic of chalcogen atoms.

Recently, we have shown that hydrosulfido-bridged dinuclear complexes $[(Cp^*MCl)_2(\mu\text{-}SH)_2]$ (M = Ru,[2] Ir (**1**), Rh:[3,4] $Cp^* = \eta^5\text{-}C_5Me_5$) are quite versatile precursors for preparing a number of μ-sulfido clusters with nuclearities ranging from 3 to 10.[2−6] These include both homometallic and heterometallic clusters, but those incorporating early transition metals are still rare. For example, complex **1** is an excellent precursor to a variety of triangular Ir_2M clusters with two capped sulfido ligands or bow-tie-type Ir_4M clusters with four capped sulfido ligands by incorporating group 8 to group 10 metals.[3,7] However, incorporation of early transition metals has not been attained.

Now we have found that employment of $[Mo(\eta^6\text{-toluene})(CO)_3]$ (**2**) as the heterometal precursor results in the formation of the desired ELHB cluster $[(Cp^*Ir)_2\{Mo(CO)_3\}(\mu_3\text{-}S)_2]$ (**3**), and this formal Mo(0) site can undergo subsequent substitution reactions as well as oxidations and reductions to give a series of new $Ir_2Mo(\mu_3\text{-}S)_2$ clusters containing various Mo centers, that is, five- to seven-coordinate Mo centers with formal oxidation states varying from 0 to +4.

Results and Discussion

Synthesis and Structure of the Ir_2Mo Sulfido-Bridged Cluster 3. Treatment of the hydrosulfido complex **1** with equimolar **2** in the presence of 2 equiv of NEt_3 at −78 °C in THF afforded the Ir_2Mo trinuclear sulfido-bridged cluster **3** in 44% yield (eq 1). Cluster **3** can be obtained only in the presence

* To whom correspondence should be addressed. Fax: +81-3-5452-6361. E-mail: ymizobe@iis.u-tokyo.ac.jp.

(1) (a) Wheatley, N.; Kalck, P. *Chem. Rev.* **1999**, *99*, 3379. (b) Hanna, T. A.; Baranger, A. M.; Bergman, R. G. *J. Am. Chem. Soc.* **1995**, *117*, 11363.

(2) Hashizume, K.; Mizobe, Y.; Hidai, M. *Organometallics* **1996**, *15*, 3303.

(3) Tang, Z.; Nomura, Y.; Ishii, Y.; Mizobe, Y.; Hidai, M. *Organometallics* **1997**, *16*, 151.

(4) Tang, Z.; Nomura, Y.; Ishii, Y.; Mizobe, Y.; Hidai, M. *Inorg. Chim. Acta* **1998**, *267*, 73.

(5) (a) Kuwata, S.; Andou, M.; Hashizume, K.; Mizobe, Y.; Hidai, M. *Organometallics* **1998**, *17*, 3429. (b) Kuwata, S.; Hashizume, K.; Mizobe, Y.; Hidai, M. *Organometallics* **2002**, *21*, 5401. (c) Hidai, M.; Kuwata, S.; Mizobe, Y. *Acc. Chem. Res.* **2000**, *33*, 46. (d) Masumori, T.; Seino, H.; Mizobe, Y.; Hidai, M. *Inorg. Chem.* **2000**, *39*, 5002. (e) Seino, H.; Masumori, T.; Hidai, M.; Mizobe, Y. *Organometallics* **2003**, *22*, 3424. (f) Kabashima, S.; Kuwata, S.; Ueno, K.; Shiro, M.; Hidai, M. *Angew. Chem., Int. Ed.* **2000**, *39*, 1128.

(6) Takagi, F.; Seino, H.; Mizobe, Y.; Hidai, M. *Organometallics* **2002**, *21*, 694.

(7) (a) Masui, D.; Ishii, Y.; Hidai, M. *Chem. Lett.* **1998**, 717. (b) Tang, Z.; Nomura, Y.; Kuwata, S.; Ishii, Y.; Mizobe, Y.; Hidai, M. *Inorg. Chem.* **1998**, *37*, 4909. (c) Kochi, T.; Nomura, Y.; Tang, Z.; Ishii, Y.; Mizobe, Y.; Hidai, M. *J. Chem. Soc., Dalton Trans.* **1999**, 2575. (d) Masui, D.; Kochi, T.; Tang, Z.; Ishii, Y.; Mizobe, Y.; Hidai, M. *J. Organomet. Chem.* **2001**, *620*, 69.

10.1021/om070190n CCC: $37.00
Publication on Web 06/05/2007

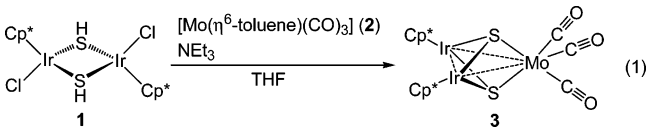

of NEt_3, presumably because the μ-sulfido complex $[(Cp^*Ir)_2(\mu_2\text{-}S)_2]$[3] as the key intermediate is generated *in situ* from **1** through dehydrochlorination. The structure of **3** has been determined unambiguously by an X-ray analysis. There are three crystallographically independent molecules in the crystal, which are separated into two types, depending on the geometry around the Mo atom, as depicted in Figure 1. Selected interatomic distances and angles are listed in Table 1.

Cluster **3** has a triangular core capped with two μ_3-sulfido ligands. Each Ir atom is bonded further to the π-Cp* group, while three terminal CO ligands are coordinated to the remaining Mo center. For the Ir_2Mo triangles, the Ir−Ir distances at 2.7696(3)−2.7877(5) Å and the Ir−Mo distances at 2.9353(7)−2.9914(9) Å are indicative of the presence of metal−metal single bonds between all metal atoms, as is usually observed for a 48-electron $M_3(\mu_3\text{-}S)_2$ core. With respect to the geometry around Mo, that in molecule 1 is a distorted trigonal bipyramid if the Ir−Mo bonds are neglected, with one CO ligand as well as one sulfide at the axial positions (S(2)−Mo(1)−C(22) angle: 177.3(2)°). The sum of the S(1)−Mo(1)−C(21), S(1)−Mo(1)−C(23), and C(21)−Mo(1)−C(23) angles at 136.4(3)°, 131.0(2)°, and 92.2(3)°, respectively, in the equatorial plane is 359.7°, indicating that these ligands and the Mo center are almost coplanar. On the other hand, the structures of molecules 2 and 3 are essentially identical, which have a crystallographic mirror plane defined by three metal atoms, and the Mo centers have a distorted square-pyramidal geometry. The apical sites are occupied by a CO ligand, whose Mo−C distances are shorter than those of the equatorial CO ligands. Deviations of the Mo centers from the least-square planes containing two equatorial C atoms and two μ_3-S atoms are 0.447(6) and 0.519(3) Å for molecules 2 and 3, respectively.

In the solid state, **3** shows four ν(C≡O) bands at 1911, 1852, 1830, and 1798 cm^{-1} in its IR spectrum, which are considerably lower than those of the starting material $[Mo(\eta^6\text{-toluene})(CO)_3]$ (**2**) at 1980 and 1910 cm^{-1}. This suggests that the metallasulfido moiety "$(Cp^*IrS)_2$" in **3** is more electron donating than η^6-toluene. As for the cubane-type clusters $[NEt_4]_3[\{Fe(SEt)\}_3\{Mo(CO)_3\}(\mu_3\text{-}S)_4]$[8] and $[(Cp^*Ir)(ReL)_2\{Mo(CO)_3\}(\mu_3\text{-}S)_4]$ (L = $S_2C_2(SiMe_3)_2$),[9] the ν(C≡O) values are reported to be 1864 and 1750 cm^{-1} for the former and 2007, 1968, and 1908 cm^{-1} for the latter. The appearance of four ν(C≡O) bands is consistent with the presence of two conformers in the solid state as revealed crystallographically. In contrast, the ^1H NMR spectrum of **3** exhibits only one singlet at δ 2.08 assignable to the Cp* ligands, indicating that the geometry around the Mo site is fluxional in solution. The oxidation state of the metals in clusters is often difficult to assign precisely; the cluster core in **3** might be described as $Ir(III)_2Mo(0)$ rather than $Ir(II)_2Mo(II)$ on the basis of the strong back-donating ability of the Mo center, as indicated by the ν(C≡O) values.

Reactions of 3 with dppe and Then with I_2. Although the carbonyl ligands in **3** hardly underwent ligand exchange reaction at room temperature, substitution of two carbonyls by $Ph_2PCH_2CH_2PPh_2$ (dppe) proceeded at 80 °C in toluene, affording

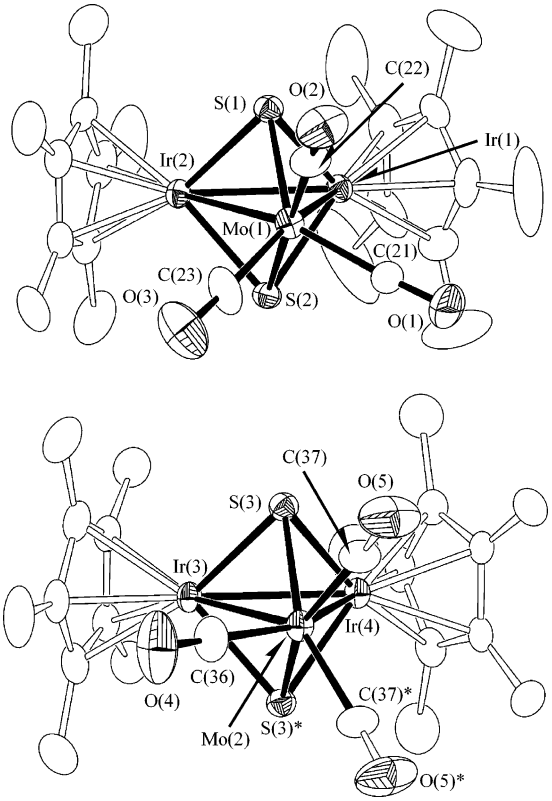

Figure 1. Molecular structures of **3**: molecule 1 (upper) and molecule 2 (lower). Hydrogen atoms are omitted for clarity.

$[(Cp^*Ir)_2\{Mo(CO)(dppe)\}(\mu_3\text{-}S)_2]$ (**4**) in moderate yield (Scheme 1). The structure of **4** has been determined by X-ray crystallography. As shown in Figure 2 and Table 2, the structure of the cluster core in **4** is analogous to that of parent **3** and as observed for molecules 2 and 3 of **3** the geometry around Mo is distorted square pyramidal with the CO ligand occupying an apical position, if the Ir−Mo bonds are ignored.

The P atoms and two sulfido ligands are deviated within 0.21 Å from the least-square plane defined by these four atoms, from which the Mo atom is separated by ca. 0.46 Å. With respect to this basal plane, the Ir(2) atom occupies the position opposite the CO ligand, and the Ir(2)−Mo distance at 3.0511(3) Å is remarkably longer than the other Ir(1)−Mo distance at 2.8487(3) Å. The ^1H NMR and $^{31}P\{^1H\}$ NMR spectra of **4** are consistent with the X-ray structure, exhibiting two singlets assignable to Cp* protons at δ 1.82 and 2.11 and one singlet for P atoms at δ 80.9. The IR spectrum of **4** exhibits a strong ν(C≡O) band at 1733 cm^{-1}, which is much lower than those of the common terminal carbonyls. Since the X-ray analysis clearly shows that the carbonyl is bound to the Mo center in a linear end-on fashion without any bridging interactions, this low ν(C≡O) value can be ascribed to the strong back-donating ability of the Mo center, which is also supported by the short Mo−CO distance at 1.897(4) Å. This ν(C≡O) value is comparable to that of molybdenum(0) diphosphine complex $[Mo(CO)(MeCN)(dppe)_2]$[10] at 1738 cm^{-1} and lower than those of monocarbonyl Mo(II)(dppe) complexes with sulfur ligands such as 1895 cm^{-1} for $[Mo(CO)(dppe)(SAr)_2]$ (Ar = 2,6-$Ph_2C_6H_3$)[11] and 1790 cm^{-1} for $[Mo(CO)(dppe)(S_2CNEt_2)_2]$.[12]

(8) Coucouvanis, D.; Al-Ahmad, S. A.; Salifoglou, A.; Papaefthymiou, V.; Kostikas, A.; Simopoulos, A. *J. Am. Chem. Soc.* **1992**, *114*, 2472.
(9) Seino, H.; Kaneko, T.; Fujii, S.; Hidai, M.; Mizobe, Y. *Inorg. Chem.* **2003**, *42*, 4585.
(10) Tatusmi, T.; Tominaga, H.; Hidai, M.; Uchida, Y. *J. Organomet. Chem.* **1980**, *199*, 63.
(11) Bishop, P. T.; Dilworth, J. R.; Nicholson, T.; Zubieta, J. *J. Chem. Soc., Dalton Trans.* **1991**, 385.
(12) Crichton, B. A.; Dilworth, J. R.; Pickett, C. J.; Chatt, J. *J. Chem. Soc., Dalton Trans.* **1981**, 892.

Table 1. Selected Interatomic Distances (Å) and Angles (deg) in 3

	molecule 1		molecule 2	molecule 3
		(a) Distances		
Ir(1)−Ir(2)	2.7696(2)	Ir(3)−Ir(4)	2.7843(5)	2.7877(5)
Ir(1)−Mo(1)	2.9353(6)	Ir(3)−Mo(2)	2.9407(9)	2.9608(9)
Ir(2)−Mo(1)	2.9908(6)	Ir(4)−Mo(2)	2.9914(9)	2.9445(9)
Ir(1)−S(1)	2.294(2)	Ir(3)−S(3)	2.292(2)	2.291(2)
Ir(1)−S(2)	2.292(2)			
Ir(2)−S(1)	2.296(2)	Ir(4)−S(3)	2.296(2)	2.297(2)
Ir(2)−S(2)	2.294(2)			
Mo(1)−S(1)	2.379(2)	Mo(2)−S(3)	2.416(2)	2.419(2)
Mo(1)−S(2)	2.435(2)			
Mo(1)−C(21)	1.965(7)	Mo(2)−C(36)	1.90(1)	1.93(1)
Mo(1)−C(22)	1.963(7)	Mo(2)−C(37)	1.995(7)	1.992(7)
Mo(1)−C(23)	1.948(8)			
C(21)−O(1)	1.149(9)	C(36)−O(4)	1.16(1)	1.16(1)
C(22)−O(2)	1.152(9)	C(37)−O(5)	1.11(1)	1.133(9)
C(23)−O(3)	1.16(1)			
		(b) Angles		
Ir(2)−Ir(1)−Mo(1)	63.16(1)	Ir(4)−Ir(3)−Mo(2)	62.93(2)	61.54(2)
Ir(1)−Ir(2)−Mo(1)	61.19(1)	Ir(3)−Ir(4)−Mo(2)	61.09(2)	62.13(2)
Ir(1)−Mo(1)−Ir(2)	55.72(1)	Ir(3)−Mo(2)−Ir(4)	55.98(2)	56.34(2)
S(1)−Ir(1)−S(2)	90.13(5)	S(3)−Ir(3)−S(3)*	90.20(5)	90.66(5)
S(1)−Ir(2)−S(2)	90.02(5)	S(3)−Ir(4)−S(3)*	90.00(5)	90.37(5)
S(1)−Mo(1)−S(2)	84.80(5)	S(3)−Mo(2)−S(3)*	84.42(6)	84.69(6)
S(1)−Mo(1)−C(21)	131.0(2)	S(3)−Mo(2)−C(37)	89.6(2)	88.4(2)
S(1)−Mo(1)−C(22)	93.0(2)	C(37)−Mo(2)−C(37)*	86.7(3)	85.5(2)
S(1)−Mo(1)−C(23)	136.4(2)	Ir(4)−Mo(2)−C(36)	149.0(3)	157.3(3)
C(21)−Mo(1)−C(23)	92.2(3)			
S(2)−Mo(1)−C(22)	177.3(2)			
Mo(1)−C(21)−O(1)	175.3(6)	Mo(2)−C(36)−O(4)	179.8(7)	177.9(9)
Mo(1)−C(22)−O(2)	177.1(6)	Mo(2)−C(37)−O(5)	176.6(7)	178.0(6)
Mo(1)−C(23)−O(3)	175.1(7)			

The CO ligand in **4** is bonded so firmly to Mo that any attempts of further substitution or removal of CO have failed.

On the other hand, treatment of **4** with I_2 afforded the monocationic Ir(III)$_2$Mo(II) cluster [(Cp*Ir)$_2${MoI(CO)(dppe)}-(μ_3-S)$_2$]I (**5**) in high yield (Scheme 1). The X-ray analysis has disclosed that the crystal contains two molecules disordered mutually only with respect to the positions of I and CO ligands, but both have a distorted trigonal prism geometry for the hexacoordinate Mo center with two basal triangles defined by P, S, and I atoms as well as P, S, and C atoms (Figure 3 and Table 3). The ^{1}H NMR spectrum of **5** exhibits two slightly broadened singlets assignable to the Cp* protons at δ 1.69 and 2.09, while the ^{31}P{^{1}H} NMR spectrum shows two doublets due to the dppe P atoms at δ 48.0 and 54.6. These NMR data are consistent with the structure of **5** in the solid state. In the IR spectrum of **5**, the ν(C≡O) band appears at 1895 cm^{-1}, which is much higher than that of **4** at 1733 cm^{-1} because of the increase in the formal oxidation state of Mo from 0 in **4** to +2 in **5** in addition to the change of the cluster charge from 0 to +1.

Oxidation Reactions of 3. When the formal Mo(0) cluster **3** was treated with 2 equiv of oxidants [Cp$_2$Fe][PF$_6$] in THF−MeCN, two-electron oxidation with concurrent loss of one of the three CO ligands occurred, yielding the dicationic cluster [(Cp*Ir)$_2${Mo(CO)$_2$(MeCN)$_2$}(μ_3-S)$_2$][PF$_6$]$_2$ (**6**) in 88% yield (Scheme 1). As depicted in Figure 4, the geometry around the formal Mo(II) center in **6** is a trigonal prism, where one basal triangle consists of one S and two carbonyl C atoms and the other contains one S and two acetonitrile N atoms. Since there exist no π-accepting CO ligands at the positions pseudo-trans to the Ir−Mo bonds (Ir(1)−Mo−C(22) angle 128.5(3)°, Ir(2)−Mo−C(21) angle 137.8(2)°), the Ir−Mo distances in **6** at 2.8594-

Scheme 1

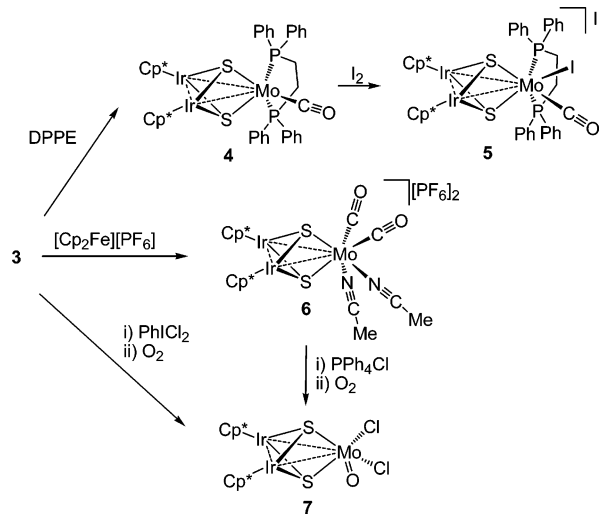

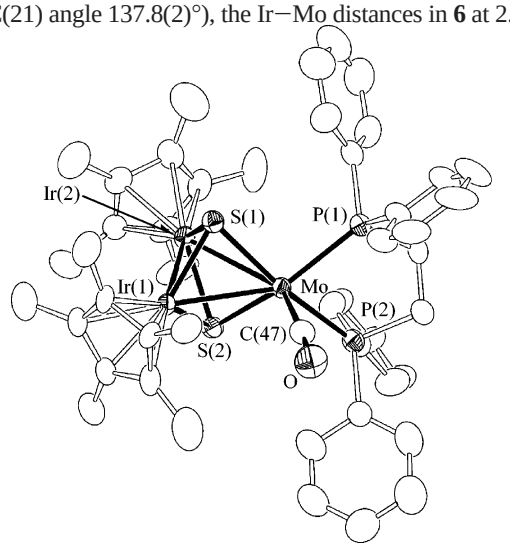

Figure 2. Molecular structure of **4**. Hydrogen atoms are omitted for clarity.

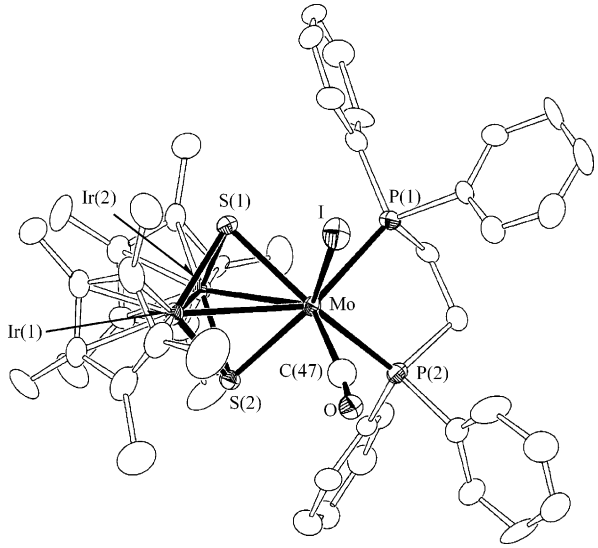

Figure 3. Structure of the cationic part of **5**·CH_2Cl_2. Hydrogen atoms are omitted for clarity. One of the two disordered molecules with higher occupancy is shown.

Table 2. Selected Interatomic Distances (Å) and Angles (deg) in 4

(a) Distances			
Ir(1)−Ir(2)	2.7223(2)	Ir(1)−Mo	2.8487(3)
Ir(2)−Mo	3.0511(3)		
Ir(1)−S(1)	2.3180(9)	Ir(1)−S(2)	2.3025(9)
Ir(2)−S(1)	2.3279(9)	Ir(2)−S(2)	2.3124(9)
Mo−S(1)	2.392(1)	Mo−S(2)	2.3492(9)
Mo−P(1)	2.445(1)	Mo−P(2)	2.419(1)
Mo−C(47)	1.897(4)	C(47)−O	1.178(5)
(b) Angles			
Ir(2)−Ir(1)−Mo	66.370(8)	Ir(1)−Ir(2)−Mo	58.803(6)
Ir(1)−Mo−Ir(2)	54.828(6)		
S(1)−Ir(1)−S(2)	90.27(3)	S(1)−Ir(2)−S(2)	89.78(3)
S(1)−Mo−S(2)	87.38(3)	S(1)−Mo−P(1)	94.85(3)
S(2)−Mo−P(2)	91.06(3)	P(1)−Mo−P(2)	79.76(3)
S(1)−Mo−C(47)	111.2(1)	S(2)−Mo−C(47)	113.4(1)
P(1)−Mo−C(47)	95.3(1)	P(2)−Mo−C(47)	81.4(1)
Ir(2)−Mo−C(47)	145.7(1)	Mo−C(47)−O	174.7(3)

(6) and 2.8962(9) Å (Table 4) are considerably shorter than the average of those in **3** at 2.9606 Å. In agreement with the solid-state structure, the ^{1}H NMR spectrum of **6** in CD_2Cl_2 shows one singlet assignable to Cp* protons at δ 2.24, together with a singlet for the Me protons of ligated MeCN molecules at δ 2.58. When dissolved in CD_3CN, the signal of MeCN shifted to the position of free MeCN, indicating that rapid exchange is occurring between coordinated and free acetonitrile molecules.

Table 3. Selected Interatomic Distances (Å) and Angles (deg) in 5·CH_2Cl_2

(a) Distances			
Ir(1)−Ir(2)	2.770(2)	Ir(1)−Mo	3.012(2)
Ir(2)−Mo	2.900(2)		
Ir(1)−S(1)	2.285(4)	Ir(1)−S(2)	2.283(3)
Ir(2)−S(1)	2.283(3)	Ir(2)−S(2)	2.282(3)
Mo−S(1)	2.392(3)	Mo−S(2)	2.367(4)
Mo−P(1)	2.528(3)	Mo−P(2)	2.554(3)
Mo−I	2.888(4)	Mo−C(47)	2.04(2)
(b) Angles			
Ir(2)−Ir(1)−Mo	60.05(5)	Ir(1)−Ir(2)−Mo	64.11(5)
Ir(1)−Mo−Ir(2)	55.84(5)		
S(1)−Ir(1)−S(2)	89.1(1)	S(1)−Ir(2)−S(2)	89.1(1)
S(1)−Mo−S(2)	84.6(1)	S(1)−Mo−P(1)	87.1(1)
S(1)−Mo−I	80.6(1)	S(2)−Mo−P(2)	89.0(1)
S(2)−Mo−C(47)	90.1(9)	P(1)−Mo−P(2)	76.5(1)
I−Mo−C(47)	74(1)	P(1)−Mo−I	80.3(1)
P(2)−Mo−C(47)	76.9(7)	Mo−C(47)−O	173.1(8)

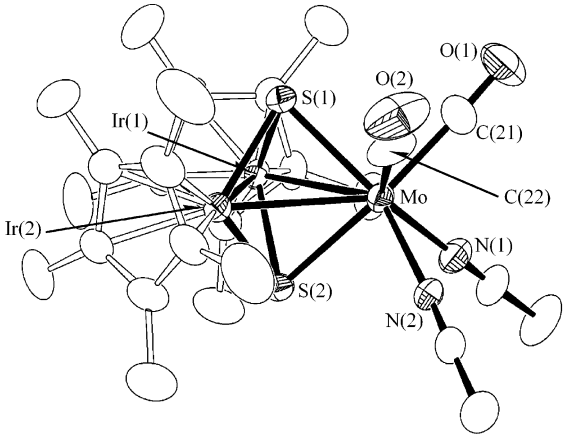

Figure 4. Structure of the cationic part of **6**·0.5MeCN. Hydrogen atoms are omitted for clarity.

Table 4. Selected Interatomic Distances (Å) and Angles (deg) in 6·0.5MeCN

(a) Distances			
Ir(1)−Ir(2)	2.7965(4)	Ir(1)−Mo	2.8962(9)
Ir(2)−Mo	2.8594(6)		
Ir(1)−S(1)	2.264(2)	Ir(1)−S(2)	2.284(2)
Ir(2)−S(1)	2.290(2)	Ir(2)−S(2)	2.273(2)
Mo−S(1)	2.371(2)	Mo−S(2)	2.431(2)
Mo−N(1)	2.170(6)	Mo−N(2)	2.171(7)
Mo−C(21)	1.963(8)	Mo−C(22)	1.99(1)
C(21)−O(1)	1.15(1)	C(22)−O(2)	1.15(1)
(b) Angles			
Ir(2)−Ir(1)−Mo	60.27(2)	Ir(1)−Ir(2)−Mo	61.59(2)
Ir(1)−Mo−Ir(2)	58.14(2)		
S(1)−Ir(1)−S(2)	91.73(7)	S(1)−Ir(2)−S(2)	91.35(5)
S(1)−Mo−S(2)	85.63(6)	S(1)−Mo−C(21)	88.2(2)
S(1)−Mo−C(22)	79.8(3)	S(2)−Mo−N(1)	84.7(2)
S(2)−Mo−N(2)	88.0(2)	N(1)−Mo−C(21)	79.4(2)
N(2)−Mo−C(22)	78.4(3)	N(1)−Mo−N(2)	77.8(2)
C(21)−Mo−C(22)	78.0(4)	Ir(1)−Mo−C(22)	128.5(3)
Ir(2)−Mo−C(21)	137.8(2)	Mo−C(21)−O(1)	175.9(8)
Mo−C(22)−O(2)	175.8(9)		

The IR spectrum of **6** exhibits two strong ν(C≡O) bands at 1946 and 2019 cm^{-1} and two weak ν(N≡C) bands at 2291 and 2321 cm^{-1}. It is to be noted that the former ν(C≡O) values are much higher than those in **3** (1911−1798 cm^{-1}), while those of the Mo(II) four-legged piano stool complexes reported previously are 1900 and 2000 cm^{-1} for [$CpMo(CO)_2(MeCN)_2$]-[PF_6][13] and 1889 and 1975 cm^{-1} for [$Cp^*Mo(CO)_2(MeCN)_2$]-[BF_4].[14]

By treatment of **6** with 0.5 equiv of oxygen gas in the presence of PPh_4Cl, the Mo center underwent coordination of two chloride ligands and monooxygenation accompanied by the elimination of the remaining CO ligands to give the neutral cluster [$(Cp^*Ir)_2(MoOCl_2)(\mu_3\text{-}S)_2$] (**7**) with the formal Mo(IV) center in 80% yield (Scheme 1). Cluster **7** can also be synthesized directly from the reaction of **3** with $PhICl_2$ prepared *in situ* from PhIO and Me_3SiCl,[15] followed by treatment with oxygen gas. In the reaction of **3** with $PhICl_2$, a two-electron-oxidized species such as [$(Cp^*Ir)_2\{MoCl_2(CO)_2\}(\mu_3\text{-}S)_2$] is probably formed initially; namely, a species was detectable that showed ν(C≡O) bands at 1905 and 1967 cm^{-1} in the IR

(13) Trieichel, P. M.; Barnett, K. W.; Shunbkin, R. L. *J. Organomet. Chem.* **1980**, *199*, 63.

(14) Benyunes, S. A.; Binelli, A.; Green, M.; Grimshire, M. *J. Chem. Soc., Dalton Trans.* **1991**, 385.

(15) (a) Blackmand, D. G.; Hodnett, N. S.; Lloyd-Jones, G. C. *J. Am. Chem. Soc.* **2006**, *128*, 7450. (b) Zefirov, N. S.; Safronov, S. O.; Kaznacheev, A. A.; Zhdankin, V. V. *Zh. Organich. Khim.* **1989**, *25*, 1807.

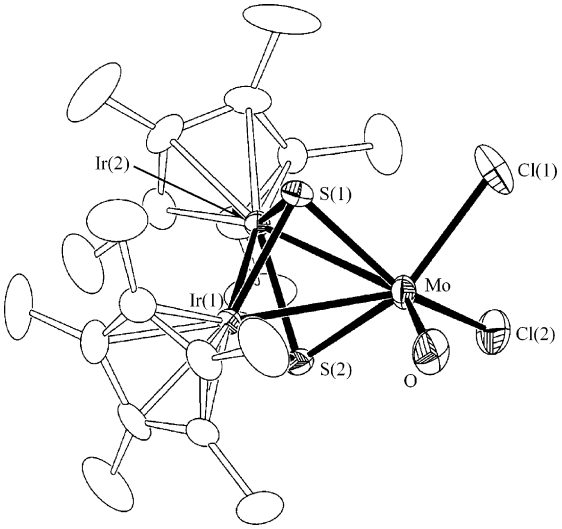

Figure 5. Molecular structure of **7**. Hydrogen atoms are omitted for clarity.

Table 5. Selected Interatomic Distances (Å) and Angles (deg) in 7

	(a) Distances		
Ir(1)−Ir(2)	2.7516(3)	Ir(1)−Mo	2.8648(7)
Ir(2)−Mo	3.0012(7)		
Ir(1)−S(1)	2.291(2)	Ir(1)−S(2)	2.293(2)
Ir(2)−S(1)	2.303(2)	Ir(2)−S(2)	2.296(2)
Mo−S(1)	2.357(2)	Mo−S(2)	2.353(2)
Mo−Cl(1)	2.403(2)	Mo−Cl(2)	2.400(3)
Mo−O	1.683(6)		
	(b) Angles		
Ir(2)−Ir(1)−Mo	64.56(2)	Ir(1)−Ir(2)−Mo	59.55(2)
Ir(1)−Mo−Ir(2)	55.89(1)		
S(1)−Ir(1)−S(2)	89.58(6)	S(1)−Ir(2)−S(2)	89.16(6)
S(1)−Mo−S(2)	86.55(7)	S(1)−Mo−Cl(1)	83.59(8)
S(2)−Mo−Cl(2)	83.02(8)	Cl(1)−Mo−Cl(2)	82.7(1)
S(1)−Mo−O	110.9(2)	S(2)−Mo−O	110.1(2)
Cl(1)−Mo−O	106.5(2)	Cl(2)−Mo−O	107.9(2)
Ir(2)−Mo−O	144.6(2)		

spectrum and Cp* resonances at δ 1.70, 1.72, 1.73, and 1.79 in the ^{1}H NMR spectrum, indicating that this species was present as a mixture of three isomers having a different coordination geometry of two CO and two Cl ligands around Mo.

The X-ray analysis disclosed the detailed structure of **7** containing a pseudo-mirror plane consisting of three metal centers (Figure 5 and Table 5). The geometry around the Mo atom is a distorted square pyramid with the O atom occupying the apical position. The Ir(2)−Mo distance at 3.0012(7) Å is significantly longer than the Ir(1)−Mo distance at 2.8648(7) Å, probably due to the strong trans influence exerted by the oxo ligand at the opposite side of Ir(2), as observed in **4**, containing the Mo center with an analogous coordination geometry. The distance of the Mo atom from the basal S_2Cl_2 plane is ca. 0.77 Å, which is longer than that in **4**.

The short Mo−O bond length at 1.683(6) Å is indicative of the presence of a Mo−O multiple bond, and the IR spectrum shows the ν(Mo═O) band at 937 cm^{-1}. Consistently, if the oxo ligand is considered to be a four-electron donor (Mo≡O), an EAN rule is satisfied for three metal centers in **7**. These values are comparable to those of the related Mo(V) complex $[Et_4N][MoOCl_2(S_2C_6H_4)]$ (1.677(2) Å, 962 cm^{-1})[16] and the Ir(III)$_2$Mo(V)$_2$ cluster $[(MoOCl_2)\{MoCl_2(dmf)\}(Cp^*Ir)_2(\mu_3\text{-}S)_4]$ (1.679(8) Å, 928 cm^{-1}).[5e] The ^{1}H NMR spectrum of **7** exhibits two singlets assignable to two inequivalent Cp* groups at δ 2.17 and 2.21.

(16) Lim, B. S.; Willer, M. W.; Miao, M.; Holm, R. H. *J. Am. Chem. Soc.* **2001**, *123*, 8343.

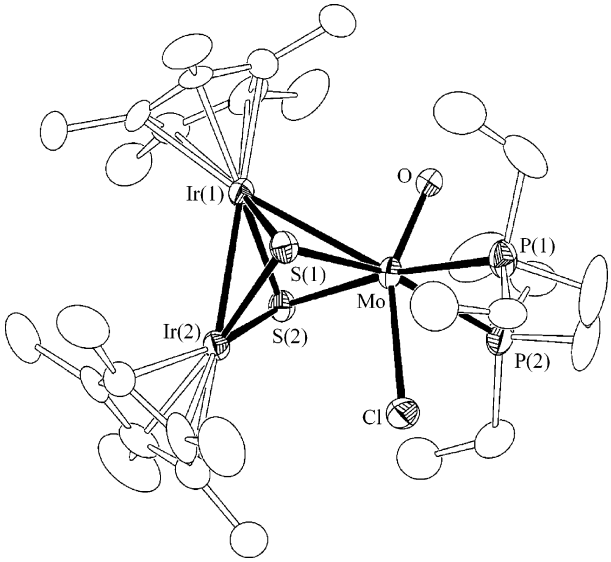

Figure 6. Structure of the cationic part of **8b**·2CH_2Cl_2. Hydrogen atoms are omitted for clarity.

Scheme 2

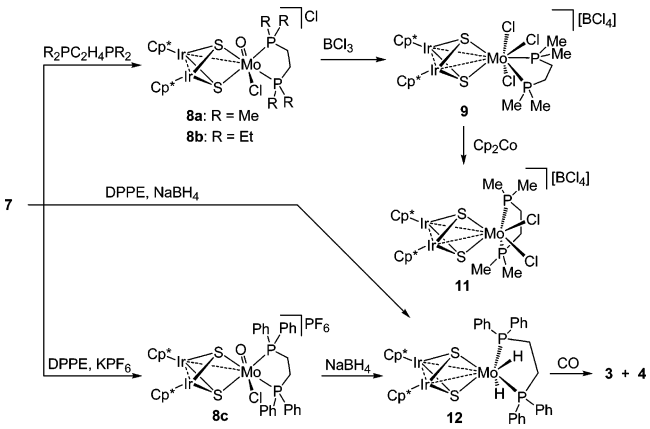

Reactions of 7 with Diphosphines. The reaction of **7** with $Me_2PCH_2CH_2PMe_2$ (dmpe) in refluxing THF or acetonitrile led to the κ^2-coordination of dmpe to give the cationic cluster $[(Cp^*Ir)_2\{MoOCl(dmpe)\}(\mu_3\text{-}S)_2]Cl$ (**8a**) in high yield (Scheme 2). The $Et_2PCH_2CH_2PEt_2$ (depe) analogue $[(Cp^*Ir)_2\{MoOCl(depe)\}(\mu_3\text{-}S)_2]Cl$ (**8b**) was obtained similarly, for which single-crystal X-ray diffraction has been undertaken.

As shown in Figure 6 and Table 6, the Mo site has a highly distorted octahedral geometry, where the two S and two P atoms occupy the equatorial plane. Both of the axial Mo−O and Mo−Cl bonds bend away from the Cp*Ir moieties with an O−Mo−Cl angle of 153.2(2)°. The oxo ligand in **8b** is again considered as a four-electron-donating ligand (Mo≡O), although the Mo−O bond distance at 1.777(6) Å is considerably elongated from that in **7** at 1.683(6) Å; namely, since the Ir(2)···Mo distance at 3.207(1) Å indicates the absence of any bonding interaction, an EAN rule is satisfied by regarding the oxo group as a four-electron donor. Indeed, the ν(Mo═O) values for **8a**, **8b**, and the dppe analogue **8c** (vide infra) at 944, 937, and 941 cm^{-1}, respectively, shift only slightly from that of **7**. For comparison, the related Mo(IV) complex $[MoOCl(dppe)_2][BPh_4]$[17] shows ν(Mo═O) at 940 cm^{-1}. The Mo−Cl bond length in **8b** at 2.563-

Table 6. Selected Interatomic Distances (Å) and Angles (deg) in 8b·2CH$_2$Cl$_2$

(a) Distances			
Ir(1)−Ir(2)	2.7530(6)	Ir(1)−Mo	2.892(1)
Ir(2)···Mo	3.207(1)		
Ir(1)−S(1)	2.306(3)	Ir(1)−S(2)	2.308(3)
Ir(2)−S(1)	2.314(3)	Ir(2)−S(2)	2.312(3)
Mo−S(1)	2.420(3)	Mo−S(2)	2.423(3)
Mo−P(1)	2.542(3)	Mo−P(2)	2.529(4)
Mo−O	1.777(6)	Mo−Cl	2.563(3)
(b) Angles			
Ir(2)−Ir(1)−Mo	69.20(2)	Ir(1)−Ir(2)−Mo	57.44(2)
Ir(1)−Mo−Ir(2)	53.36(2)		
S(1)−Ir(1)−S(2)	88.4(1)	S(1)−Ir(2)−S(2)	88.1(1)
S(1)−Mo−S(2)	83.2(1)	S(1)−Mo−P(1)	96.7(1)
S(2)−Mo−P(2)	97.6(1)	P(1)−Mo−P(2)	80.3(1)
S(1)−Mo−P(2)	164.5(1)	S(2)−Mo−P(1)	171.8(1)
S(1)−Mo−O	110.3(2)	S(2)−Mo−O	105.6(2)
P(1)−Mo−O	82.2(2)	P(2)−Mo−O	84.5(2)
S(1)−Mo−Cl	89.4(1)	S(2)−Mo−Cl	94.4(1)
P(1)−Mo−Cl	77.3(1)	P(2)−Mo−Cl	75.1(1)
O−Mo−Cl	153.2(2)		

(3) Å is much longer than that in **7** at 2.400(3) and 2.403(2) Å due to the trans influence of the oxo ligand.

The ^{1}H NMR spectrum of **8a** shows two signals for the inequivalent Cp* protons at δ 1.99 and 2.07 together with two doublets each integrated to 6H, assignable to the Me protons in dmpe at δ 1.68 and 1.72, respectively. The equivalent P atoms resonate at δ 39.1 in the ^{31}P{^{1}H} NMR spectrum.

In contrast, the reaction of **7** with dppe did not proceed under the conditions forming **8a** and **8b**. However, the reaction did proceed in the presence of KPF_6 in THF at reflux to afford the dppe analogue [(Cp*Ir)$_2${MoOCl(dppe)}(μ_3-S)$_2$][PF$_6$] (**8c**) in good yield (Scheme 2). The ^{1}H NMR and ^{31}P{^{1}H} NMR spectra of **8c** are diagnostic of the structure for **8a** and **8b**.

Removal of the Oxo Ligand from 8a. Since the Ir$_2$Mo clusters with the Mo center without the CO ligands have been derivatized successfully, their reduction to the clusters containing a low-valent Mo center has been attempted. Although reductions of certain Mo(VI) or Mo(V) oxo complexes by deoxygenation reaction using PPh_3 have been reported,[18] direct reduction with the elimination of the oxo ligands from the Mo(IV) center is not precedented. We therefore attempted the conversion of the oxo ligand in **8** into the Cl ligands prior to the chemical reductions. However, treatment of **8a** with Me_3SiCl,[19] one of the most popular reagents for substituting the oxo ligands by Cl, did not work. On the other hand, **8a** did react with BCl_3 to give the cluster without an oxo ligand, [(Cp*Ir)$_2${MoCl$_3$(dmpe)}(μ_3-S)$_2$][BCl$_4$] (**9**), in 80% yield (Scheme 2). In the course of the reaction, one molecule of BCl_3 abstracts the oxo ligand and chlorinates the Mo center, and the other BCl_3 forms the BCl_4^- anion by reacting with the outer Cl^- anion of **8a**. Figure 7 shows the X-ray structure of **9**, having the molybdenum site with a capped trigonal prism geometry, where the phosphorus atom P(1) caps the rectangle consisting of three Cl atoms and P(2). Pertinent bond distances and angles in **9** are listed in Table 7. It is noteworthy that seven-coordinate Mo complexes with a capped trigonal prism geometry are still rare, precedented examples of which are, for example, [Mo(CN^{t}Bu)$_7$][PF$_6$]$_2$,[20] [Mo(CF$_3$COO)$_2$(CO)$_2$(PMe$_3$)$_3$],[21] and [MoX$_2$(CO)$_2$(κ^2-dppm)(κ^1-dppm)] (dppm = $Ph_2PCH_2PPh_2$, X = I (**10**), NCS).[22]

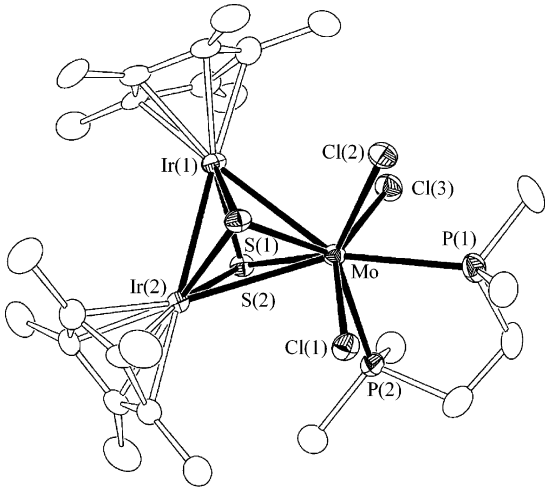

Figure 7. Structure of the cationic part of **9**. Hydrogen atoms are omitted for clarity.

Table 7. Selected Interatomic Distances (Å) and Angles (deg) in 9

(a) Distances			
Ir(1)−Ir(2)	2.7661(4)	Ir(1)−Mo	2.8769(8)
Ir(2)−Mo	3.0525(7)		
Ir(1)−S(1)	2.264(2)	Ir(1)−S(2)	2.279(2)
Ir(2)−S(1)	2.260(2)	Ir(2)−S(2)	2.279(2)
Mo−S(1)	2.382(2)	Mo−S(2)	2.384(2)
Mo−P(1)	2.641(2)	Mo−P(2)	2.550(2)
Mo−Cl(1)	2.474(2)	Mo−Cl(2)	2.519(2)
Mo−Cl(3)	2.457(2)		
(b) Angles			
Ir(2)−Ir(1)−Mo	65.46(2)	Ir(1)−Ir(2)−Mo	59.02(2)
Ir(1)−Mo−Ir(2)	55.52(2)		
S(1)−Ir(1)−S(2)	88.68(7)	S(1)−Ir(2)−S(2)	88.76(7)
S(1)−Mo−S(2)	83.54(7)	S(1)−Mo−P(1)	134.14(8)
S(1)−Mo−Cl(1)	79.66(8)	S(1)−Mo−Cl(2)	74.43(7)
S(2)−Mo−P(1)	142.31(7)	S(2)−Mo−P(2)	76.61(7)
S(2)−Mo−Cl(3)	79.76(7)	P(2)−Mo−Cl(1)	78.86(7)
Cl(2)−Mo−Cl(3)	84.72(8)	P(2)−Mo−Cl(3)	83.77(7)
Cl(1)−Mo−Cl(2)	93.78(8)	P(1)−Mo−P(2)	73.71(7)
P(1)−Mo−Cl(1)	76.32(8)	P(1)−Mo−Cl(2)	68.90(7)
P(1)−Mo−Cl(3)	74.44(8)		

Although the ^{31}P{^{1}H} NMR spectrum of **9** shows two sharp doublets at δ 37.9 and 78.3, the ^{1}H NMR spectrum recorded at room temperature is elusive except for the appearance of one broad Cp* signal. However, the spectrum recorded at −40 °C exhibited four doublets assignable to the Me protons of dmpe along with two singlets due to the Cp* groups (Figure 8). Because the ^{31}P{^{1}H} NMR spectra are essentially identical in these temperature range, this fluxional behavior might be explained by the pivotal rotation of the $Cl_3P(2)$ square around the fixed Mo−P(1) axis. This pseudorotation proceeds probably through a capped octahedral intermediate, as illustrated in Scheme 3. In contrast, for the dppm complex **10** one of the iodo ligands is present at the capped position and its fluxional behavior is presumed to arise from the dissociation of the capped iodo ligand or the simple exchange between the capped iodine atom and the edge iodine atom.[22b]

(17) Levason, W.; McAuliffe, C. A.; Sayle, B. J. *J. Chem. Soc., Dalton Trans.* **1976**, 1177.

(18) Berg, J. M.; Holm, R. H. *J. Am. Chem. Soc.* **1984**, *106*, 3035.

(19) (a) Nielson, A. J.; Glenny, M. W.; Rickard, C. E. F.; Waters, J. M. *J. Chem. Soc., Dalton. Trans.* **2000**, 4569. (b) Rufanov, K. A.; Zarubin, D. N.; Usynyuk, N. A.; Gourevitch, D. N.; Sundermeyer, J.; Churakov, A. V.; Howard, J. A. K. *Polyhedron* **2001**, *20*, 379. (c) Siemeling, U.; Kölling, L.; Kuhnert, O.; Neumann, B.; Stammler, A.; Stammler, H. G.; Fink, G.; Kaminski, E.; Kiefer, A.; Schrock, R. R. *Z. Anorg. Allg. Chem.* **2003**, *629*, 781. (d) Janas, Z.; Jerzykiewicz, L. B.; Richards, R. L.; Sobota, P. *Inorg. Chim. Acta* **2003**, *350*, 379.

(20) Lewis, D. L.; Lippard, S. J. *J. Am. Chem. Soc.* **1975**, *97*, 2697.

(21) Beauchamp, A.; Belanger-gariepy, F.; Arabi, S. *Inorg. Chem.* **1985**, *24*, 1860.

(22) (a) Blagg, A.; Hutton, A. T.; Shaw, B. L. *Polyhedron* **1987**, *6*, 95. (b) Cotton, F. A.; Matusz, M. *Polyhedron* **1987**, *6*, 261.

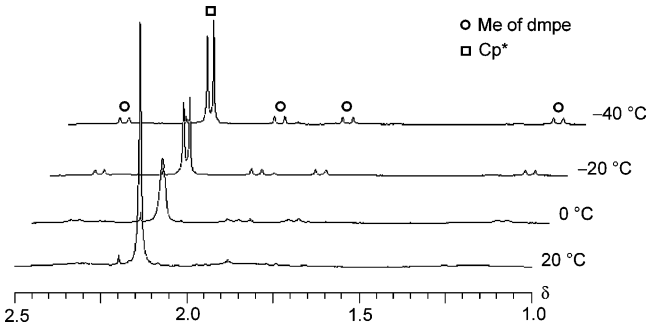

Figure 8. VT NMR spectrum of **9**.

Scheme 3

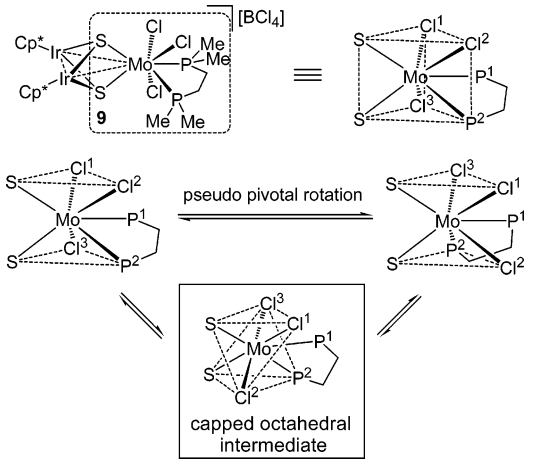

Treatment of **9** with Cp_2Co was also carried out, which afforded only a one-electron-reduction product, the paramagnetic cluster $[(Cp^*Ir)_2\{MoCl_2(dmpe)\}(\mu_3\text{-}S)_2][BCl_4]$ (**11**), in moderate yield (Scheme 2). The atom-connecting scheme and the presence of one BCl_4^- anion for **11** were confirmed by the preliminary X-ray analysis. The six-coordinate molybdenum center adopts the trigonal prism structure, in which the basal triangles both consist of one Cl, one P, and one S.

Hydride Reduction of 8c. Since reduction of **8a** via the electron donation of **9** gave only the one-electron-reduction product **11**, the hydridic reduction of **8** has been attempted. Although the reaction of **8a** with $NaBH_4$ gave no tractable products, that of **8c** took place to yield the expected dihydrido cluster $[(Cp^*Ir)_2\{MoH_2(dppe)\}(\mu_3\text{-}S)_2]$ (**12**) in good yield (Scheme 2). It has also been found that **12** can be prepared directly from **7** upon treating with $NaBH_4$ in the presence of dppe. The structure of **12** has been unambiguously determined by X-ray crystallography, as shown in Figure 9 and Table 8, whereby two hydrides have been located in the Fourier map and refined successfully. The structure around Mo is a trigonal prism, as observed for **5**, **6**, and **11**, but it is to be noted that each of the two phosphorus atoms of dppe bind diagonally to the rectangular P_2H_2 face in **12**. The IR spectrum of **12** displays the ν(Mo−H) bands at 1742 and 1702 cm^{-1}, while ^1H NMR spectrum at 20 °C shows one pseudotriplet assignable to hydrido protons. The VT NMR spectra indicate the fluxional behavior in the NMR time scale, which is ascribable to a pseudorotation of the P_2H_2 square or a site exchange of two hydrides. Thus, the hydrido protons were recorded as a complicated signal characteristic of the HH′PP′ system at −60 °C, which turned to an ideal triplet corresponding to the H_2P_2 pattern at 80 °C (Figure 10). It is noteworthy that although the Ru_3 cluster $[(Cp^*Ru)_2\{RuH(PPh_3)_2\}(\mu_2\text{-}H)(\mu_3\text{-}S)_2]$[5a] (**13**) has essentially the same ligand set and hence the same electron count of 48 as **12**,

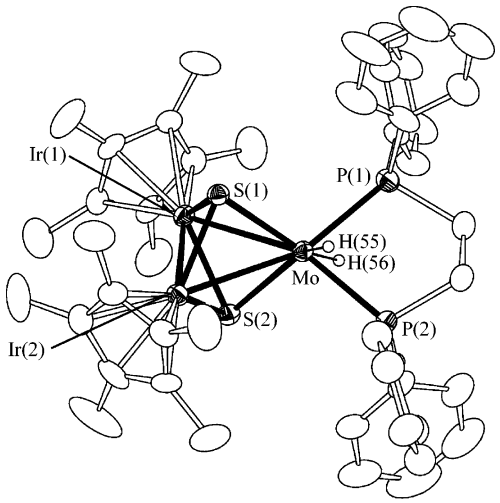

Figure 9. Molecular structure of **12**. Hydrogen atoms except for hydrido ligands and solvating THF molecule are omitted for clarity. Only one of the disordered Ph groups bound to P(2) is shown.

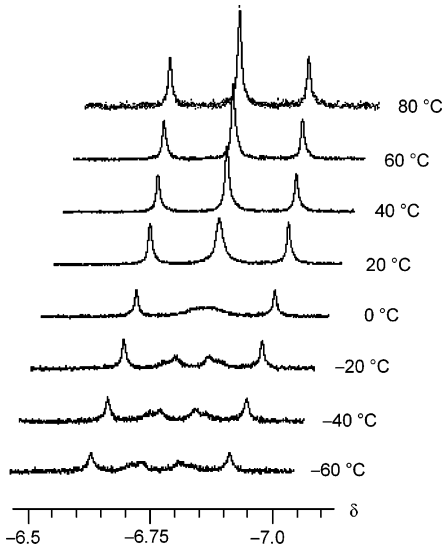

Figure 10. VT NMR spectrum of the hydrido region for **12**.

Table 8. Selected Interatomic Distances (Å) and Angles (deg) in 12·THF

(a) Distances			
Ir(1)−Ir(2)	2.7227(4)	Ir(1)−Mo	2.9149(7)
Ir(2)−Mo	2.9645(7)		
Ir(1)−S(1)	2.299(2)	Ir(1)−S(2)	2.313(2)
Ir(2)−S(1)	2.309(2)	Ir(2)−S(2)	2.305(2)
Mo−S(1)	2.347(2)	Mo−S(2)	2.350(2)
Mo−P(1)	2.377(2)	Mo−P(2)	2.375(2)
Mo−H(55)	1.64(7)	Mo−H(56)	1.76(6)
(b) Angles			
Ir(2)−Ir(1)−Mo	63.34(1)	Ir(1)−Ir(2)−Mo	61.49(2)
Ir(1)−Mo−Ir(2)	55.17(2)		
S(1)−Ir(1)−S(2)	89.57(6)	S(1)−Ir(2)−S(2)	89.52(6)
S(1)−Mo−S(2)	87.51(6)	S(1)−Mo−P(1)	107.73(7)
S(1)−Mo−H(55)	137(2)	S(2)−Mo−P(2)	84.7(2)
S(2)−Mo−H(56)	135(2)	P(1)−Mo−H(56)	68(2)
P(2)−Mo−H(55)	67(2)	P(1)−Mo−H(55)	80(2)
P(2)−Mo−H(56)	77(2)		

the $Ru(PPh_3)_2$ center in **13** adopts an octahedral geometry with mutually trans terminal and bridging hydrido ligands. In the related 50-electron cluster $[(Cp^*Ir)_2\{Ru(dppe)\}(\mu_2\text{-}H)_2(\mu_3\text{-}S)_2]$,[7c] having an Ir_2Ru core with two metal−metal single bonds, the Ru center is also octahedral and two mutually trans hydrido ligands are both bridging the Ru−Ir bonds.

Table 9. Crystal Data for 3, 4, 5·CH_2Cl_2, and 6·0.5MeCN

	3	**4**	**5**·CH_2Cl_2	**6**·0.5MeCN
formula	$C_{23}H_{30}Ir_2MoO_3S_2$	$C_{47}H_{54}Ir_2MoOP_2S_2$	$C_{48}H_{56}Cl_2I_2Ir_2MoOP_2S_2$	$C_{27}H_{37.5}F_{12}Ir_2MoN_{2.5}O_2P_2S_2$
fw	898.99	1241.39	1580.13	1263.54
space group	*Pnma* (No. 62)	$P2_1/c$ (No. 14)	$P\bar{1}$ (No. 1)	$P\bar{1}$ (No. 2)
a, Å	18.1741(5)	19.5871(9)	10.636(2)	10.467(3)
b, Å	27.3477(8)	10.8158(5)	11.495(2)	12.988(3)
c, Å	21.2134(5)	21.2531(9)	12.161(2)	16.240(4)
α, deg	90	90	64.897(6)	70.917(9)
β, deg	90	93.573(1)	75.099(7)	77.63(1)
γ, deg	90	90	84.534(7)	72.61(1)
V, Å^3	10543.5(5)	4493.7(3)	1300.9(4)	1974.6(8)
Z	16	4	1	2
ρ_{calcd}, g cm^{-3}	2.265	1.835	2.017	2.125
μ(Mo Kα), mm^{-1}	10.748	6.397	6.819	7.326
cryst size, mm^3	0.50 × 0.20 × 0.15	0.40 × 0.30 × 0.30	0.20 × 0.10 × 0.10	0.30 × 0.20 × 0.20
no. of unique reflns	12 301 (R_{int} = 0.071)	10 254 (R_{int} = 0.030)	8000 (R_{int} = 0.033)	8665 (R_{int} = 0.026)
no. of data obsd	7380 ($F_o^2 > 2\sigma(F_o^2)$)	8459 ($F_o^2 > 2\sigma(F_o^2)$)	6238 ($F_o^2 > 2\sigma(F_o^2)$)	5867 ($F_o^2 > 2\sigma(F_o^2)$)
no. of variables	657	551	595	496
transmn factor	0.097−0.199	0.092−0.147	0.360−0.506	0.146−0.231
R_1[a]	0.030	0.026	0.033	0.036
wR_2[b]	0.086	0.063	0.096	0.084
GOF[c]	1.026	1.013	1.071	1.010

[a] $R_1 = \sum||F_o| - |F_c||/\sum|F_o|$ (observed data). [b] $wR_2 = [\sum(w(F_o^2 - F_c^2)^2)/\sum w(F_o^2)^2]^{1/2}$ (all data). [c] GOF = $[\sum w(|F_o| - |F_c|)^2/\{$(no. observed) − (no. variables)$\}]^{1/2}$.

Table 10. Crystal Data for 7, 8b·2CH_2Cl_2, 9, and 12·THF

	7	**8b**·2CH_2Cl_2	**9**	**12**·THF
formula	$C_{20}H_{30}Cl_2Ir_2MoOS_2$	$C_{32}H_{58}Cl_6Ir_2MoOP_2S_2$	$C_{26}H_{46}BCl_7Ir_2MoP_2S_2$	$C_{50}H_{64}Ir_2MoOP_2S_2$
fw	901.86	1277.98	1224.08	1287.50
space group	$P2_1/c$ (No. 14)	$P2_1/n$ (No. 14)	$P\bar{1}$ (No. 2)	*Pbcn* (No. 60)
a, Å	14.356(2)	11.036(3)	8.753(1)	24.372(3)
b, Å	10.192(1)	26.998(7)	14.128(2)	22.530(3)
c, Å	18.080(2)	15.173(4)	16.135(1)	17.977(2)
α, deg	90	90	91.099(6)	90
β, deg	107.881(2)	96.372(1)	96.240(6)	90
γ, deg	90	90	99.605(6)	90
V, Å^3	2517.7(5)	4493(2)	1954.3(4)	9871(2)
Z	4	4	2	8
ρ_{calcd}, g cm^{-3}	2.379	1.889	2.080	1.733
μ(Mo Kα), mm^{-1}	11.452	6.745	7.812	5.828
cryst size, mm^3	0.20 × 0.10 × 0.10	0.30 × 0.20 × 0.15	0.50 × 0.10 × 0.05	0.25 × 0.15 × 0.10
no. of unique reflns	5764 (R_{int} = 0.045)	10 275 (R_{int} = 0.089)	8566 (R_{int} = 0.034)	11 302 (R_{int} = 0.078)
no. of data obsd	3072 ($F_o^2 > 2\sigma(F_o^2)$)	3882 ($F_o^2 > 2\sigma(F_o^2)$)	5579 ($F_o^2 > 2\sigma(F_o^2)$)	6453 ($F_o^2 > 2\sigma(F_o^2)$)
no. of variables	283	473	416	557
transmn factor	0.193−0.318	0.150−0.364	0.337−0.677	0.319−0.558
R_1[a]	0.027	0.043	0.037	0.043
wR_2[b]	0.065	0.160	0.124	0.088
GOF[c]	1.007	1.009	1.005	1.030

[a] $R_1 = \sum||F_o| - |F_c||/\sum|F_o|$ (observed data). [b] $wR_2 = [\sum(w(F_o^2 - F_c^2)^2)/\sum w(F_o^2)^2]^{1/2}$ (all data). [c] GOF = $[\sum w(|F_o| - |F_c|)^2/\{$(no. observed) − (no. variables)$\}]^{1/2}$.

It has been reported that the isoelectronic cluster **13** is converted to the dicarbonyl cluster [(Cp*Ru)$_2${Ru(CO)$_2$(PPh$_3$)}-(μ_3-S)$_2$] under 1 atm of CO at 50 °C. Under a CO atmosphere at room temperature, **12** gave a mixture of **3** and **4** in the ratio of 54:46 from the NMR criteria (Scheme 2).

In conclusion, we have synthesized the ELHB $Ir_2Mo(\mu_3\text{-}S)_2$ cluster **3** containing a formal zerovalent $Mo(CO)_3$ fragment and demonstrated the pathways to derivatize a series of $Ir_2Mo(\mu_3\text{-}S)_2$ clusters starting from **3**, which include direct or consecutive reactions such as ligand exchange, oxidation, and reduction at the Mo site. It should be emphasized that the molybdenum site incorporated in the cluster core adopts a wide range of oxidation states or coordination numbers and geometries in these clusters. Further transformations are now under investigation to generate clusters with more reactive, coordinatively unsaturated Mo centers that can activate certain small molecules.

Experimental Section

General Procedures. All manipulations were performed under a nitrogen atmosphere using standard Schlenk techniques. Solvents were dried by common procedures. Complexes **1**[3] and **2**[23] were prepared according to the literature methods, while other reagents were obtained commercially and used as received. The ^{1}H NMR (400 MHz) and ^{31}P{^{1}H} NMR (162 MHz) spectra were recorded on a JEOL alpha-400 spectrometer at 20 °C, whose chemical shifts were referred to the residual ^{1}H impurities of the solvents or external 85% H_3PO_4, respectively. The IR spectra were obtained on a JASCO FT/IR-420 spectrometer. Elemental analyses were done with a Perkin-Elmer 2400 series II CHN analyzer.

Preparation of [(Cp*Ir)$_2${Mo(CO)$_3$}(μ_3-S)$_2$] (3). To a THF solution (8 mL) of **1** (61 mg, 0.077 mmol) were added NEt_3 (21 μL, 15 mg, 0.151 mmol) and then a THF solution (3 mL) of [Mo(η^6-toluene)(CO)$_3$] (20 mg, 0.075 mmol) at −78 °C, and the mixture was gradually warmed to room temperature with stirring. After 24 h, the resultant dark red suspension was evaporated *in vacuo*, and the residue was extracted with THF. The extract was dried and the residue was crystallized from CH_2Cl_2−ether to give dark red crystals of **3** (30 mg, 44% yield). ^{1}H NMR (CD_2Cl_2): δ

(23) Nesmeyanov, A. N.; Krivykh, V. V.; Kaganovich, V. S.; Rybinskaya, M. I. *J. Organomet. Chem.* **1975**, *102*, 185.

2.08 (s, 30H, Cp*). IR (KBr, cm^{-1}): ν(C≡O), 1911s, 1852s, 1830s, 1798s. Anal. Calcd for $C_{23}H_{30}Ir_2MoO_3S_2$: C, 30.73; H, 3.36. Found: C, 30.73; H, 3.54.

Preparation of [(Cp*Ir)$_2${Mo(CO)(dppe)}(μ_3-S)$_2$] (4). A mixture of **3** (358 mg, 0.398 mmol) and dppe (163 mg, 0.410 mmol) in toluene (30 mL) was stirred for 4 h at 80 °C, and the resultant mixture was filtered. Addition of hexane to the concentrated filtrate gave **4** as dark brown crystals (335 mg, 68% yield). ^{1}H NMR (C_6D_6): δ 1.82, 2.11 (s, 15H each, Cp*), 2.34−2.48, 2.82−2.97 (m, 2H each, CH_2), 6.96−7.45, 8.18−8.22 (m, 20H, Ph). ^{31}P{^{1}H} NMR (C_6D_6): δ 80.9 (s). IR (KBr, cm^{-1}): ν(C≡O), 1733s. Anal. Calcd for $C_{47}H_{54}Ir_2MoOP_2S_2$: C, 45.47; H, 4.38. Found: C, 45.80; H, 4.32.

Preparation of [(Cp*Ir)$_2${MoI(CO)(dppe)}(μ_3-S)$_2$]I (5). Into a benzene solution (5 mL) of **4** (66 mg, 0.053 mmol) was added I_2 (15 mg, 0.058 mmol) dissolved in benzene (5 mL) at room temperature. The mixture turned immediately to a brown suspension, which was stirred continuously for 2 h. The resultant suspension was filtered off and the remaining solid was dried *in vacuo*. Crystallization from CH_2Cl_2−hexane gave the product as dark brown crystals formulated to be **5**·CH_2Cl_2 (67 mg, 80% yield). ^{1}H NMR (CD_3CN): δ 1.69, 2.09 (br s, 15H each, Cp*), 2.00−2.40 (m, 4H, CH_2), 5.43 (s, 2H, CH_2Cl_2), 7.13−8.26 (m, 20H, Ph). ^{31}P{^{1}H} NMR (CD_3CN): δ 48.0, 54.6 (d, J_{P-P} = 35 Hz, 1P each). IR (KBr, cm^{-1}): ν(C≡O), 1895s. Anal. Calcd for $C_{48}H_{56}Cl_2I_2Ir_2MoOP_2S_2$: C, 36.49; H, 3.57. Found: C, 36.16; H, 3.51.

Preparation of [(Cp*Ir)$_2${Mo(CO)$_2$(MeCN)$_2$}(μ_3-S)$_2$][PF$_6$]$_2$ (6). To a THF−MeCN solution (300 mL/100 mL) of **3** (2.585 g, 2.875 mmol) was added a MeCN (100 mL) solution of [Cp_2Fe][PF_6] (1.906 g, 5.758 mmol) at −78 °C, and the mixture was gradually warmed to room temperature. The resultant dark brown suspension was dried *in vacuo*, and the residue was washed with ether (80 mL and 20 mL × 3) to remove Cp_2Fe. Crystallization from MeCN−ether gave dark brown crystals of **6**·0.5MeCN (3.214 g, 88% yield). ^{1}H NMR (CD_2Cl_2): δ 1.97 (s, 1.5H, free MeCN), 2.24 (s, 30H, Cp*), 2.58 (s, 6H, coordinated MeCN). IR (KBr, cm^{-1}): ν(C≡N), 2321 m, 2291 m; ν(C≡O), 2019s, 1946s. Anal. Calcd for $C_{27}H_{37.5}F_{12}Ir_2MoN_{2.5}O_2P_2S_2$: C, 25.67; H, 2.99; N, 2.77. Found: C, 25.65; H, 2.92; N, 2.66.

Preparation of [(Cp*Ir)$_2$(MoOCl$_2$)(μ_3-S)$_2$] (7). Method A. A mixture (40 mL) of **6**·0.5MeCN (1.063 g, 0.842 mmol) and PPh_4Cl (639 mg, 1.70 mmol) in CH_2Cl_2 (40 mL) was stirred for 12 h at room temperature. After adding O_2 (12 mL, 0.488 mmol) by syringe to the reaction atmosphere, the solution was stirred continuously for 12 h. Addition of hexane to the concentrated extract afforded **7** as dark red crystals (604 mg, 80% yield). ^{1}H NMR ($CDCl_3$): δ 2.17, 2.21 (s, 15H each, Cp*). IR (KBr, cm^{-1}): ν(Mo═O), 937m. Anal. Calcd for $C_{20}H_{30}Cl_2Ir_2MoOS_2$: C, 26.64; H, 3.35. Found: C, 26.87; H, 3.42.

Method B. A CH_2Cl_2 solution (10 mL) of $PhICl_2$ prepared from PhIO (59 mg, 0.270 mmol) and Me_3SiCl (70 μL, 0.552 mmol) at −78 °C was added into a CH_2Cl_2 solution (20 mL) of **3** (233 mg, 0.260 mmol), and the mixture was gradually warmed to room temperature with stirring. After 12 h, the resulting mixture was degassed and then stirred under O_2 for 3 h. Addition of hexane to the concentrated extract gave **7** as dark red crystals (143 mg, 61% yield).

Preparation of [(Cp*Ir)$_2${MoOCl(dmpe)}(μ_3-S)$_2$]Cl (8a). A MeCN solution (5 mL) of **7** (67 mg, 0.074 mmol) and dmpe (13 μL, 12 mg, 0.080 mmol) was stirred for 1 h at reflux. The resulting mixture was filtered and the filtrate was dried *in vacuo*. The residue was extracted with CH_2Cl_2 (3 mL), and hexane was added to the extract to form very efflorescent dark red crystals, which were collected and dried thoroughly *in vacuo* to give **8a** (62 mg, 80% yield). ^{1}H NMR ($CDCl_3$): δ 1.68, 1.72 (d, J_{P-H} = 10.0 Hz, 6H each, Me of dmpe), 1.99, 2.07 (s, 15H each, Cp*), 2.00−2.55 (m, 4H, CH_2). ^{31}P{^{1}H} NMR ($CDCl_3$): δ 39.1 (s). IR (KBr, cm^{-1}): ν(Mo═O), 944m. Anal. Calcd for $C_{26}H_{46}Cl_2Ir_2MoOP_2S_2$: C, 29.68; H, 4.41. Found: C, 30.01; H, 4.42.

Preparation of [(Cp*Ir)$_2${MoOCl(depe)}(μ_3-S)$_2$]Cl (8b). This compound was prepared from **7** (29 mg, 0.032 mmol) and depe (10 μL, 9.0 mg, 0.043 mmol) in the same manner as described for **8a**. Crystallization of the product from CH_2Cl_2−hexane afforded **8b**·2CH_2Cl_2 as dark red crystals (14 mg, 60% yield). ^{1}H NMR ($CDCl_3$): δ 1.18−1.30 (m, 12H, C*H*$_3$CH$_2$ of depe), 1.89−2.01 (m, 8H, CH$_3$C*H*$_2$ of depe), 2.05, 2.10 (s, 15H each, Cp*), 5.31 (s, 4H, CH_2Cl_2). ^{31}P{^{1}H} NMR ($CDCl_3$): δ 60.6 (s). IR (KBr, cm^{-1}): ν(Mo═O), 937m. Anal. Calcd for $C_{32}H_{58}Cl_6Ir_2MoOP_2S_2$: C, 30.07; H, 4.57. Found: C, 30.45; H, 4.51.

Preparation of [(Cp*Ir)$_2${MoOCl(dppe)}(μ_3-S)$_2$][PF$_6$] (8c). A THF suspension (5 mL) containing **7** (55 mg, 0.061 mmol), dppe (26 mg, 0.066 mmol), and KPF_6 (23 mg, 0.126 mmol) was stirred for 5 h at reflux. The resulting suspension was dried *in vacuo*, and the residue was extracted with CH_2Cl_2 (3 mL). Addition of hexane to the extract afforded **8c**·CH_2Cl_2 as dark red crystals (69 mg, 75% yield). ^{1}H NMR ($CDCl_3$): δ 2.00, 2.11 (s, 15H each, Cp*), 2.81−3.13 (m, 4H, CH_2), 5.31 (s, 2H, CH_2Cl_2), 7.33−7.67 (m, 20H, Ph). ^{31}P{^{1}H} NMR ($CDCl_3$): δ 45.5 (br s). IR (KBr, cm^{-1}): ν(Mo═O), 941m. Anal. Calcd for $C_{47}H_{56}Cl_3F_6Ir_2MoOP_3S_2$: C, 37.77; H, 3.78. Found: C, 38.02; H, 3.78.

Preparation of [(Cp*Ir)$_2${MoCl$_3$(dmpe)}(μ_3-S)$_2$][BCl$_4$] (9). Into a CH_2Cl_2 solution (30 mL) of **8a** (542 mg, 0.515 mmol) was added BCl_3 in heptane (1.0 M, 1.2 mL, 1.2 mmol) at −78 °C, and the mixture was gradually warmed to room temperature with stirring. The resultant red suspension was dried and the residue was crystallized from CH_2Cl_2−hexane to give **9** as dark brown crystals (504 mg, 80% yield). ^{1}H NMR ($CDCl_3$ at 20 °C): δ 2.17 (br s, Cp*). ^{1}H NMR (CD_2Cl_2 at −40 °C): δ 2.08, 2.10 (s, 15H each, Cp*), 1.07, 1.69, 1.89, 2.34 (d, J_{P-H} = 11.7 Hz, 3H each, Me of dmpe) 2.00−2.50 (m, 4H, CH_2). ^{31}P{^{1}H} NMR (CD_2Cl_2): δ 37.9, 78.3 (d, J_{P-P} = 61 Hz, 1P each). Anal. Calcd for $C_{26}H_{46}BCl_7Ir_2MoP_2S_2$: C, 25.51; H, 3.79. Found: C, 25.41; H, 3.77.

Preparation of [(Cp*Ir)$_2${MoCl$_2$(dmpe)}(μ_3-S)$_2$][BCl$_4$] (11). Into a CH_2Cl_2 solution (5 mL) of **9** (40 mg, 0.033 mmol) was added Cp_2Co (7 mg, 0.04 mmol) at −78 °C, and the mixture was gradually warmed to room temperature. The resultant dark brown solution was dried and the residue was crystallized from THF−hexane to give **11**·THF as dark brown crystals (22 mg, 56% yield). Anal. Calcd for $C_{30}H_{54}BCl_6Ir_2MoOP_2S_2$: C, 28.58; H, 4.32. Found: C, 28.21; H, 4.00.

Preparation of [(Cp*Ir)$_2${MoH$_2$(dppe)}(μ_3-S)$_2$] (12). Method A. An EtOH (50 mL) suspension of **8c**·CH_2Cl_2 (751 mg, 0.502 mmol) and excess $NaBH_4$ (685 mg, 18.1 mmol) was stirred for 3 h at room temperature. The resulting suspension was dried *in vacuo* and the residue was extracted with toluene (40 mL + 10 mL × 3). Evaporation of toluene from combined extracts gave **12** as a dark brown powder (432 mg, 71% yield). ^{1}H NMR (C_6D_6): δ −6.79 (br t, J_{P-H} = 59 Hz, 2H, MoH), 1.76 (s, 30H, Cp*), 1.83−2.39 (m, 4H, CH_2), 6.85−7.66 (m, 20H, Ph). ^{31}P{^{1}H} NMR (C_6D_6): δ 87.3 (s). IR (KBr, cm^{-1}): ν(Mo−H), 1742m, 1702m. Anal. Calcd for $C_{46}H_{56}Ir_2MoP_2S_2$: C, 45.46; H, 4.64. Found: C, 45.44; H, 4.61. Single crystals of **12**·THF suitable for an X-ray analysis were grown by slow evaporation of a THF−hexane solution of **12**. Anal. Calcd for $C_{50}H_{64}Ir_2MoOP_2S_2$ (**12**·THF): C, 46.64; H, 5.01. Found: C, 46.42; H, 4.86.

Method B. An EtOH (100 mL) suspension of **7** (1.247 g, 1.383 mmol), dppe (552 mg, 1.39 mmol), and excess $NaBH_4$ (555 mg, 14.7 mmol) was stirred for 3 h at room temperature. A similar workup to that of method A gave **12** (1.406 g, 84% yield).

X-ray Crystallography. The X-ray analyses of **3**, **4**, **5**·CH_2Cl_2, **6**·0.5MeCN, **7**, **8b**·2CH_2Cl_2, **9**, and **12**·THF were carried out at room temperature on a Rigaku Mercury-CCD diffractometer equipped with a graphite-monochromatized Mo Kα source. Data collection was performed by using the CrystalClear program

package.[24] All data were corrected for Lorentz and polarization effects as well as absorption. Details are listed in Tables 9 and 10.

Structure solution and refinements were conducted by using the CrystalStructure program package.[25] The positions of non-hydrogen atoms were determined by Patterson methods (PATTY)[26] except for **3**, for which direct methods have been employed (SHELX-97),[27] and subsequent Fourier synthesis (DIRDIF99).[28] These were refined anisotropically except for those stated below. In **5**, there existed two disordered molecules in the crystal with the occupancies of 0.65 and 0.35, which differ mutually about the positions of I and CO ligands. Disorder was also found for the orientation of one Ph group attached to P(2) in **12** with a ratio of 1:1. As for the non-hydrogen atoms in the disordered CO ligands and solvating CH_2Cl_2 in **5**·CH_2Cl_2 and those of a disordered Ph group bound to P(2) and solvating THF in **12**, refinements were done with isotropic thermal parameters. The absolute structure of **5**·CH_2Cl_2 was confirmed by the Flack parameter of 0.007(6). Hydrogen atoms were placed at ideal positions and included at the final stages of refinements with fixed parameters, while the hydrido ligands in **12** were found in the Fourier map and refined isotropically.

(24) *CrystalClear 1.3.5*; Rigaku Corporation, 1999. *CrystalClear Software User's Guide*; Molecular Structure Corporation, 2000. Pflugrath J. W. *Acta Crystallogr., Sect. D* **1999**, *55*, 1718.

(25) *CrystalStructure 3.8.0*, Crystal Structure Analysis Package; Rigaku and Rigaku/MSC, 2000−2006. Carruthers, J. R.; Rollett, J. S.; Betteridge, P. W.; Kinna, D.; Pearce, L.; Larsen, A.; Gabe, E. *CRYSTALS Issue 11*; Chemical Crystallography Laboratory: Oxford, U.K., 1999.

(26) PATTY: Beurskens, P. T.; Admiraal, G.; Beurskens, G.; Bosman, W. P.; Garcia-Granda, S.; Gould, R. O.; Smits, J. M. M.; Smykall, C. *The DIRDIF Program System*; Technical Report of the Crystallography Laboratory; University of Nijmegen: Nijmegen, The Netherlands, 1992.

(27) SHELX-97: Sheldrick, G. M. *SHELX-97*, Program for the Refinement of Crystal Structures; University of Göttingen: Göttingen, Germany, 1997.

(28) DIRDIF-99: Beurskens, P. T.; Admiraal, G.; Beurskens, G.; Bosman, W. P.; de Gelder, R.; Israel, R.; Smits, J. M. M. *The DIRDIF-99 Program System*; Technical Report of the Crystallography Laboratory; University of Nijmegen: Nijmegen, The Netherlands, 1999.

Acknowledgment. This work was supported by a Grant-in-Aid for Scientific Research on Priority Areas (No. 14078206, "Reaction Control of Dynamic Complexes", and No. 18065005, "Chemistry of Concerto Catalysis") from the Ministry of Education, Culture, Sports, Science and Technology, Japan, and by CREST of JST (Japan Science and Technology Agency).

Supporting Information Available: Detailed results of X-ray crystallography for **3**, **4**, **5**·CH_2Cl_2, **6**·0.5MeCN, **7**, **8b**·$2CH_2Cl_2$, **9**, and **12**·THF are available in CIF format. This material is available free of charge via the Internet at http://pubs.acs.org.

OM070190N